**Figure 4**

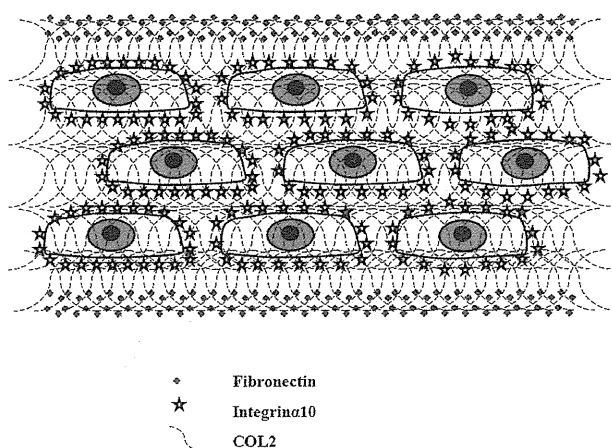
**Immunohistochemical examination: fluorescence microscopy of layered chondrocyte sheets.** Fibronectin (shown in green) was detected in the periphery of the triple-layered chondrocyte sheets (A, D). However, collagen type II (shown in green) was located in the pericellular matrix of the triple-layered chondrocyte sheets (B, E) and integrin  $\alpha 10$  (shown in green) was scattered diffusely throughout the triple-layered chondrocyte sheets (C, F). The blue color shows counterstained DNA. DAPI excites at about 360 nm and emits at about 460 nm when bound to DNA, producing a blue fluorescence. A, B, C: Scale bar = 20  $\mu\text{m}$ . D, E, F: Scale bar = 2  $\mu\text{m}$

reflected in their characteristic adhesiveness. The flat bottoms of the culture dish and the effects of gravity during the culture period may also fashion this even surface texture.

The concept of the chondron was first introduced by Benninghoff in 1925, with the chondrocyte and its pericellular capsules together representing the chondron, historically considered the primary structural, functional, and metabolic unit of articular and other hyaline cartilages.[16] During recent decades, many researchers have investigated and established the molecular anatomy, functional properties, and metabolic contribution of the chondron in articular cartilage homeostasis and its failure during the initiation and progression of degenerative osteoarthritis. It is interesting that SEM evaluations of the basal aspect of the cell sheets suggest that chondrocytes with ECM, chondrons, were embedded in opposing sides

of the sheet surfaces. Although chondrons were only faintly observed because of the thick ECM, it is clear that our sheets contain the basic structural, functional, and metabolic units of articular cartilage and it is expected that they will maintain their function of reduction of friction and the transmission of load. It is thus suggested that, using our technique, these triple-layered chondrocyte sheets have substantially reconstructed the ordinary superficial zone of articular cartilage. To our knowledge, this is the first report of the morphologic evaluation of the bottom aspect of cultivated chondrocytes, which was made possible because the cell sheets were harvested as a single contiguous shape using a noninvasive method without enzyme digestion, thus keeping their original structure.

In this study, the properties of the chondrocyte sheets were investigated, including the expression and localiza-



**Figure 5**  
**Schematic illustration of the distribution pattern of extracellular adhesion molecules in triple-layered chondrocyte sheets.** Fibronectin was located peripherally in the triple-layered chondrocyte sheet and integrin  $\alpha 10$  was observed close to the chondrocytes, in the pericellular matrix, in the layered construct. However, collagen type II was scattered diffusely throughout the layered cell sheets.

tion of SOX9, COL1, 2, 27, integrin  $\alpha 10$  and fibronectin. SOX9 has recently been shown to be involved in the control of cell-specific activation of COL2A1 in chondrocytes and to directly regulate the type II collagen gene *in vivo*. [17] Therefore, the high mobility group protein SOX9 is emerging as a key regulator of chondrogenesis. Moreover, Jenkins *et al.* recently reported that the newest cartilage collagen gene, COL27A1, contains two enhancer elements that bind SOX9. [18] Integrin  $\alpha 10$  is specifically

expressed in chondrocytes. Chondrocytes, depending on the species and tissue origin, express a characteristic set of integrins, including receptors for collagen type II ( $\alpha 1\beta 1$ ,  $\alpha 2\beta 1$ , and  $\alpha 10\beta 1$ ), fibronectin ( $\alpha 5\beta 1$ ,  $\alpha v\beta 3$ ,  $\alpha v\beta 5$ ), and laminin ( $\alpha 6\beta 1$ ). Among these receptors, integrin  $\alpha 10\beta 1$  is the major integrin mediating chondrocyte-collagen interactions in cartilage. [19,20] Compared with chondrocytes in conventional monolayer culture and single chondrocyte sheets, the significantly higher expression of SOX9 and COL27 mRNA in the layered chondrocyte sheets revealed characteristics more closely resembling normal chondrocyte differentiation, which implies the maintenance of a phenotype. In addition, significantly higher expression of fibronectin and integrin  $\alpha 10$  mRNA in the layered chondrocyte sheets also demonstrated the adhesiveness of the cell sheets. Furthermore, on immunohistochemical examination, the expression of fibronectin and integrin  $\alpha 10$  in the layered chondrocyte cell sheets verified this adhesiveness and illustrated the specific cartilaginous phenotype of the cell sheets. In both this study and in earlier results using temperature-responsive surfaces [14] it was possible to recover monolayer cell sheets together with deposited fibronectin. Fibronectin matrix adhering to the basal side of cell sheets can function as a glue to attach cell sheets onto other surfaces. [14] In fact, cell sheets recovered from temperature-responsive surfaces easily adhere to other surfaces. [21] Interestingly, as illustrated by the immunohistochemical results in this study (Fig. 5), fibronectin was detected peripherally on both sides of the triple-layered chondrocyte sheets, not only on the basal aspect as described previously [14] but also on the top side, while showing intense adhesiveness on the basal side only. It is possible to hypothesize that the culture period prolonged by 1 week with a cell-culture

**Table 1: List of primers used in the real-time PCR.**

Primer ID	Accession No.	Sequence	Expect size(bp)
Collagen Type I-F Collagen Type I-R	NM_000088	AAG GGT GAG ACA GGC GAA CAA TTG CCA GGA GAA CCA GCA AGA	170
Collagen Type II-F Collagen Type II-R	NM_033150	GGA CTT TTC TTC CCT CTC T GAC CCG AAG GGT CTT ACA GGA	113
SOX9-F SOX9-R	NM_000346	AAC GCC GAG CTC AGC AAG A CCG CGG CTG GTA CTT GTA ATC	138
Collagen27 $\alpha$ 1-F Collagen27 $\alpha$ 1-R	NM_032888	GGG CCT TAT GGA AAT CCA GGT C GGT CCA GGA TAG CCC TTG TGT C	176
Integrin $\alpha$ 10-F Integrin $\alpha$ 10-R	NM_003637	CTG GGA TAT GTG CCC GTG TG TTG GAG CCA TCC AAG ACA ATG A	112
Fibronectin I-F Fibronectin I-R	NM_001030524	GCA CAG GGG AAG AAA AGG AG TTG AGT GGA TGG GAG GAG AG	189

**Table 2: Results of the post hoc test (Scheffe's method).**

Dependent variable	(I) VI	(J) VI	Difference of averages (I-J)	SEM	P-value	95% CI		Figure 3
						Lower limit	Upper limit	
COL1	Mono	Cell Sheet	.05250	.05374	.635	-.1043	.2093	
		Layered	.39500*	.05374	.000	.2382	.5518	*1
	Cell Sheet	Mono	-.05250	.05374	.635	-.2093	.1043	
		Layered	.34250*	.05374	.000	.1857	.4993	*2
	Layered	Mono	-.39500*	.05374	.000	-.5518	-.2382	*1
		Cell Sheet	-.34250*	.05374	.000	-.4993	-.1857	*2
COL2	Mono	Cell Sheet	-.12750	.05183	.099	-.2787	.0237	
		Layered	-.52500*	.05183	.000	-.6762	-.3738	*3
	Cell Sheet	Mono	.12750	.05183	.099	-.0237	.2787	
		Layered	-.39750*	.05183	.000	-.5487	-.2463	*4
	Layered	Mono	.52500*	.05183	.000	.3738	.6762	*3
		Cell Sheet	.39750*	.05183	.000	.2463	.5487	*4
SOX9	Mono	Cell Sheet	.04500	.08833	.880	-.2127	.3027	
		Layered	-.68500*	.08833	.000	-.9427	-.4273	*5
	Cell Sheet	Mono	-.04500	.08833	.880	-.3027	.2127	
		Layered	-.73000*	.08833	.000	-.9877	-.4723	*6
	Layered	Mono	.68500*	.08833	.000	.4273	.9427	*5
		Cell Sheet	.73000*	.08833	.000	.4723	.9877	*6
COL27	Mono	Cell Sheet	-.13250	.17224	.751	-.6350	.3700	
		Layered	-.43750	.17224	.088	-.9400	.0650	*7
	Cell Sheet	Mono	.13250	.17224	.751	-.3700	.6350	
		Layered	-.30500	.17224	.260	-.8075	.1975	
	Layered	Mono	.43750	.17224	.088	-.0650	.9400	*7
		Cell Sheet	.30500	.17224	.260	-.1975	.8075	
Integrin a10	Mono	Cell Sheet	.05500	.10949	.883	-.2645	.3745	
		Layered	-.36500*	.10949	.027	-.6845	-.0455	*8
	Cell Sheet	Mono	-.05500	.10949	.883	-.3745	.2645	

**Table 2: Results of the post hoc test (Scheffe's method).** (Continued)

		Layered	-.42000*	.10949	.013	-.7395	-.1005	*9
	Layered	Mono	.36500*	.10949	.027	.0455	.6845	*8
		Cell Sheet	.42000*	.10949	.013	.1005	.7395	*9
Fibronectin	Mono	Cell Sheet	-.71500*	.16992	.007	-1.2108	-.2192	*10
		Layered	-.93000*	.16992	.001	-1.4258	-.4342	*11
	Cell Sheet	Mono	.71500*	.16992	.007	.2192	1.2108	*10
		Layered	-.21500	.16992	.479	-.7108	.2808	
	Layered	Mono	.93000*	.16992	.001	.4342	1.4258	*11
		Cell Sheet	.21500	.16992	.479	-.2808	.7108	

insert may affect the localization of fibronectin. In this period, the fibronectin could either be moved from its position in the single-layer cell sheets or be newly secreted in areas of contact with the insert. However, the exact mechanism underlying this phenomenon is unclear in our results and further research into this is required.

It is inevitable that for medical applications and when using vital cells such as in ACI, preparation times, including *in vitro* culture periods, will need to be shortened. Overall, it is important to be able to reduce the chondrocyte culture time before cell-sheet harvesting, with reduced time for cell expansion and ECM production, but without changing the extra week of culture to reinforce the cell sheets as this prolonged step is substantially beneficial to this new strategy to cure OA using bioengineered chondrocyte sheets.

In conventional ACI[6] for cartilage regeneration, transplanted periosteal patches, which are used to enclose the implanted chondrocytes, sometimes cause hypertrophy of the regenerated chondral surface. Some improved methods use alternative scaffolds such as collagen membranes, hyaluronan polymers, and atelocollagen gels.[7,22] In comparison to these conventional ACI techniques, the cell-sheet technology has the specific advantage of generating three-dimensional tissues fabricated by autologous cells without using a scaffold while also showing intense adhesiveness on the basal side. The advantages of such cell sheets are that it is easy to culture and expand, and, most importantly, they have good adhesion and barrier function.[9] This means they can protect against intra-articular catabolic factors and prevent proteoglycan escape from the injured site. Moreover, these cell sheets are considered to contain an advantageous supply of growth factors. Furthermore, such cell sheets could be useful as an alternative to the periosteum itself, which is usually used in ACI. Although cell sheets have good adhesive properties com-

pared with other applications using cell-sheet techniques, such as in the cornea and heart, transplanted chondrocyte sheets will be exposed to a harsh environment resulting from weight bearing and friction. Development of new devices to prevent the sheets peeling from the transplanted site is indispensable to future clinical application.

Although focal gene delivery using a cell sheet has not been addressed in this paper, this may also have clinical potential for treatment of cartilage degeneration. The development of a therapeutic apparatus to deliver the cell sheet to the injured site less invasively may therefore be fundamental to expanding its use in the treatment of patients demonstrating the early stages of osteoarthritis.

The results of this study therefore lead to a new strategy for cartilage regeneration using novel bioengineered chondrocyte sheets produced using a cell-sheet technique.

## Conclusion

These experiments demonstrated that triple-layered chondrocyte sheets contain the phenotypic markers COL2, COL27, SOX9, and the adhesion molecules integrin  $\alpha 10$  and fibronectin. Cell-sheet technology therefore provides particular advantages for cartilage regeneration, giving three-dimensional tissue constructed without a scaffold and with good adhesiveness to both itself and to an injured cartilage site.

## Methods

### Preparation of human chondrocytes

This study was performed in compliance with the Helsinki Declaration, and was approved by the Institutional Review Board for Clinical Research of Tokai University School of Medicine (ref. 04-056).

Human chondrocytes were obtained from the knee joints of young athletes who underwent anterior cruciate liga-

ment reconstruction at Tokai University Oiso hospital from December 2004 to April 2006. Twenty-nine knees from 29 patients aged 14 to 49 years (21 males and 8 females) were used as the source of these cells. All subjects provided informed consent. The specimens were stored in basal medium (BM) containing Dulbecco's modified Eagle's medium/F12 (DMEM/F12; GIBCO, Invitrogen Corporation, Carlsbad, CA, USA) supplemented with 10% heat-inactivated fetal bovine serum (FBS; GIBCO) and 50 µg/ml ascorbic acid (Wako Pure Chemical Industries, Ltd, Osaka, Japan) and 1% antibiotic-antimycotic mixture (ABAM; 10,000 U/ml penicillin G, 10,000 µg/ml streptomycin sulfate, and 25 µg/ml amphotericin B as Fungizone; GIBCO) until required for the next step. The cartilage samples were cut into small pieces. Thereafter, minced specimens were digested for 1 hr in BM containing 0.4% Pronase E (Kaken Pharmaceutical Inc., Tokyo, Japan), and for a further 4 hrs in BM containing 0.016% Collagenase P (Roche Diagnostics GmbH, Mannheim, Germany). The digested cell suspension was passed through a cell strainer (BD Falcon™; BD Bioscience, Bedford, MA, USA) with a pore size of 100 µm, and the isolated cells rinsed twice with chilled Dulbecco's phosphate-buffered saline (PBS; Dainippon Pharmaceutical Co., Osaka, Japan). The chondrocytes were then seeded into 500 cm<sup>2</sup> square dishes (245 × 245 mm; Corning Inc., Corning, NY, USA) at a density of 10,000 cells/cm<sup>2</sup> and cultured in BM with 20% FBS (GIBCO) at 37°C in an atmosphere of 5% CO<sub>2</sub> and 95% air (according to the method of Sato *et al.*).[23]

#### **Temperature-responsive culture dishes**

The specific procedures for the preparation of temperature-responsive culture dishes (provided by CellSeed, Inc) have all been previously described.[24] Briefly, *N*-isopropylacrylamide (IPAAm) monomer solution was spread onto commercial tissue-culture polystyrene dishes. These dishes were then subjected to electron beam irradiation, thus resulting in polymerization and covalent binding of the IPAAm to the dish surface. Poly-IPAAm (PIPAAm)-grafted dishes were rinsed with cold distilled water to remove any ungrafted IPAAm. Finally, the culture dishes were sterilized using ethylene oxide gas.

#### **Preparation of conventional monolayer cultures of chondrocytes and single-layer chondrocyte sheets**

To detach the primary passage cells, chondrocytes were digested using 0.05% trypsin:EDTA (GIBCO), and then counted using a hemacytometer. For the conventional monolayer culture, cartilage cells were seeded into culture dishes (diameter: 35 mm, Iwaki Glass Company, LTD., Tokyo, Japan) at a density of 1,000 cells/cm<sup>2</sup>. To prepare the single-layer chondrocyte sheets, resuspended chondrocytes were seeded at a density of 10,000 cells/cm<sup>2</sup> in UpCell culture dishes (diameter: 35 mm, provided by CellSeed, Inc.). The seeded chondrocytes were cultured in

BM adjusted to 20% FBS (GIBCO) at 37°C in an atmosphere of 5% CO<sub>2</sub> and 95% air. At 100% confluence, the cultured cells were harvested and prepared for gene expression analysis.

The samples in conventional culture were harvested with a sterile cell scraper. To release confluent cells as a monolayer chondrocyte sheet from the UpCell temperature-responsive culture dishes, the dishes were removed from the incubator and let stand at about 25°C for 30 min. The culture medium was then removed from the dish, and the cell sheet harvested using polyvinylidene difluoride (PVDF) membrane as a supporting membrane. The lifted chondrocyte sheet edges promptly attached to the overlaid supporting membrane, and the cell sheet and PVDF membrane film were gently detached from the UpCell dish.

#### **Fabrication of cell sheet into three-layer sheets of chondrocytes**

Each cell sheet prepared as above was transferred onto another confluent chondrocyte sheet to fabricate multilayered sheets. Because the multilayered sheets spontaneously floated in culture medium, a 0.4 µm cell culture insert (Falcon, Becton Dickinson, NJ, USA) was placed on top to prevent floating, and then culture of the sheets was continued for 1 week to obtain firm and perfect integration of the cells in the multilayer chondrocyte sheets.

#### **Scanning electron microscopy evaluation**

Triple-layered chondrocyte cell sheets were soaked in 0.1 mol/l phosphate buffer and 2% glutaraldehyde for 2 h. Next, the samples were fixed in 1% osmium solution for 1 h and dehydrated in ascending concentrations of ethanol (50%, 70%, 80%, 90%, 95%, and 100%). The specimens were dried using the critical point drying method, sputter-coated with gold, and affixed to an adhesive interface for observation by SEM (JSM-840; Jeol Ltd., Tokyo, Japan). Both the top and bottom surfaces of the cell sheets were observed.

#### **RNA isolation and cDNA synthesis**

Total RNA extraction was carried out using the RNeasy Mini kit (Qiagen Inc., Valencia, CA) according to the manufacturer's instructions. RNA quality from each sample was determined using the A260/280 absorbance ratio and by electrophoresis on 1.2% agarose formaldehyde gel. Total RNA (1.0–2.0 µg) was reverse transcribed into single stand cDNA using MuLV reverse transcriptase (Applied Biosystems, Foster City, CA, USA). The reverse-transcription reaction was performed in a thermocycler at 42°C for 60 min and then at 95°C for 5 min.

#### **Primer design and real-time PCR**

All oligonucleotide primer sets were designed based upon published mRNA sequences. The expected amplicon

lengths ranged from 70 to 200 bp. The oligonucleotide primers used in this study are listed in Table 1. The real-time PCR was performed in a SmartCycler™ (Cepheid, Sunnyvale, CA, USA) using SYBR Green PCR Master Mix (Applied Biosystems). From 2 to 2.5 µl of cDNA template was used for real-time PCR in a final volume of 25 µl. cDNA was amplified according to the following condition: 95 °C for 15 s and 60 °C for 60 s from 35 to 45 amplification cycles. Fluorescence changes were monitored with SYBR Green after every cycle. A melting curve analysis was performed (a 0.5 °C/s increase from 55 to 95 °C with continuous fluorescence readings) at the end of cycles to ensure that single PCR products were obtained. The amplicon size and reaction specificity were confirmed by 2.5% agarose gel electrophoresis. All reactions were repeated in six separate PCR runs using RNA isolated from four sets of human samples. The results were evaluated using the SmartCycler™ software program. Glyceraldehyde-3-phosphate dehydrogenase (GAPDH) primers were used to normalize samples. To monitor crossover contaminations of PCR, RNase-free water (Qiagen Inc) was included in the RNA extraction and was used as a negative control. To ensure the quality of the data, a negative control was always included in each run.

#### Immunohistochemical staining

Frozen sections (30 × 24 × 5 mm) of triple-layered cell sheets were prepared using OCT compound (Sakura Fine Technical Co., Tokyo, Japan). The sections were then washed in PBS, and were reacted at room temperature for 60 min with three monoclonal antibodies: an anti-fibronectin mouse monoclonal antibody (clone FBN11, diluted 1:500, #MS-1351-P0; Thermo SCIENTIFIC, Lab Vision Co., CA, USA), an anti-human CD11c (integrin α10) mouse monoclonal antibody (clone BU15, diluted 1:200, #SM1834PS; Acris Antibodies GmbH, Herford, Germany), and an anti-human collagen type 2 mouse monoclonal antibody (clone α-4C11, diluted to 5 µg/ml, #F-57; Daiichi Fine Chemical Co., Toyama, Japan). The sections were washed in PBS, and reacted with polyclonal rabbit anti-mouse immunoglobulin/FITC, diluted 1:100 (#F0261; DAKOCytomation, Glostrup, Denmark) as a fluorescent secondary antibody. Mounting with a water-soluble mounting medium (VECTASHIELD® Mounting Medium with DAPI, Vector Laboratories, Inc., Burlingame, CA, USA) was performed to counterstain DNA after washing sections in purified water.

#### Statistical analysis

The real-time PCR results are expressed as the mean ± standard error of the mean from six determinations and representative results are shown. The statistical software program SPSS (Version 17.0, SPSS, Chicago, IL, USA) was used to perform standard analysis of variance and the Scheffe's post hoc test. Table 2 lists the p-values shown in Figure 3.

#### Authors' contributions

GM, MS, NK, MK, and TK performed the research. JIL, MI, HS, and JM analyzed the data. HS provided the temperature-responsive culture dishes for these experiments. NO took charge of the statistical analyses. GM, JIL, MS, and JM wrote the manuscript. All authors have read and approved the final manuscript.

#### Acknowledgements

We thank Professor Teruo Okano, Dr. Tatsuya Shimizu, and Dr. Masayuki Yamato (Institute of Advanced Biomedical Engineering and Science, Tokyo Women's Medical University) for their useful comments and technical criticism. This work was supported by the Takeda Science Foundation, The General Insurance Association of Japan, Mitsui Sumitomo Insurance Welfare Foundation, High-Tech Research Center Project 2004 for Private Universities and a Grant-in-Aid for Scientific Research from the Ministry of Education, Culture, Sports, Science and Technology and the Ministry of Health, Labour and Welfare of Japan.

#### References

- Mankin HJ: **The response of articular cartilage to mechanical injury.** *J Bone Joint Surg Am* 1982, **64(3)**:460-466.
- Buckwalter JA, Mankin HJ: **Articular cartilage: degeneration and osteoarthritis, repair, regeneration, and transplantation.** *Instr Course Lect* 1998, **47**:487-504.
- Kim HK, Moran ME, Salter RB: **The potential for regeneration of articular cartilage in defects created by chondral shaving and subchondral abrasion. An experimental investigation in rabbits.** *J Bone Joint Surg Am* 1991, **73(9)**:1301-1315.
- Steadman JR, Rodkey WG, Singleton SB, Briggs KK: **Microfracture technique for full-thickness chondral defect: technique and clinical results.** *Operative Techniques in Orthopaedics* 1997, **7**:4300-4304.
- Marcacci M, Kon E, Zaffagnini S, Iacono F, Neri MP, Vascellari A, Visani A, Russo A: **Multiple osteochondral arthroscopic grafting (mosaicplasty) for cartilage defects of the knee: prospective study results at 2-year follow-up.** *Arthroscopy* 2005, **21(4)**:462-470.
- Brittberg M, Lindahl A, Nilsson A, Ohlsson C, Isaksson O, Peterson L: **Treatment of deep cartilage defects in the knee with autologous chondrocyte transplantation.** *N Engl J Med* 1994, **331(14)**:889-895.
- Masuoka K, Asazuma T, Ishihara M, Sato M, Hattori H, Yoshihara Y, Matsui T, Takase B, Kikuchi M, Nemoto K: **Tissue engineering of articular cartilage using an allograft of cultured chondrocytes in a membrane-sealed atelocollagen honeycomb-shaped scaffold (ACHMS scaffold).** *J Biomed Mater Res B Appl Biomater* 2005, **75(1)**:177-184.
- Okano T, Yamada N, Sakai H, Sakurai Y: **A novel recovery system for cultured cells using plasma-treated polystyrene dishes grafted with poly(N-isopropylacrylamide).** *J Biomed Mater Res* 1993, **27(10)**:1243-1251.
- Kaneshiro N, Sato M, Ishihara M, Mitani G, Sakai H, Mochida J: **Bio-engineered chondrocyte sheets may be potentially useful for the treatment of partial thickness defects of articular cartilage.** *Biochem Biophys Res Commun* 2006, **349(2)**:723-731.
- Nishida K, Yamato M, Hayashida Y, Watanabe K, Maeda N, Watanabe H, Yamamoto K, Nagai S, Kikuchi A, Tano Y, et al.: **Functional bio-engineered corneal epithelial sheet grafts from corneal stem cells expanded ex vivo on a temperature-responsive cell culture surface.** *Transplantation* 2004, **77(3)**:379-385.
- Shimizu T, Yamato M, Itoi Y, Akutsu T, Setomaru T, Abe K, Kikuchi A, Umezumi M, Okano T: **Fabrication of pulsatile cardiac tissue grafts using a novel 3-dimensional cell sheet manipulation technique and temperature-responsive cell culture surfaces.** *Circ Res* 2002, **90(3)**:e40.
- Shimizu T, Sekine H, Yang J, Itoi Y, Yamato M, Kikuchi A, Kobayashi E, Okano T: **Polysurgery of cell sheet grafts overcomes diffusion limits to produce thick, vascularized myocardial tissues.** *FASEB J* 2006, **20(6)**:708-10.
- Harimoto M, Yamato M, Hirose M, Takahashi C, Itoi Y, Kikuchi A, Okano T: **Novel approach for achieving double-layered cell**

- sheets co-culture: overlaying endothelial cell sheets onto monolayer hepatocytes utilizing temperature-responsive culture dishes. *J Biomed Mater Res* 2002, **62(3)**:464-470.
14. Kushida A, Yamato M, Konno C, Kikuchi A, Sakurai Y, Okano T: **Temperature-responsive culture dishes allow nonenzymatic harvest of differentiated Madin-Darby canine kidney (MDCK) cell sheets.** *J Biomed Mater Res* 2000, **51(2)**:216-223.
  15. Hughes LC, Archer CW, ap Gwynn I: **The ultrastructure of mouse articular cartilage: collagen orientation and implications for tissue functionality. A polarised light and scanning electron microscope study and review.** *Eur Cell Mater* 2005, **9**:68-84.
  16. Poole CA: **Articular cartilage chondrons: form, function and failure.** *J Anat* 1997, **191(Pt 1)**:1-13.
  17. Wenke AK, Rothhammer T, Moser M, Bosserhoff AK: **Regulation of integrin alpha10 expression in chondrocytes by the transcription factors AP-2epsilon and Ets-1.** *Biochem Biophys Res Commun* 2006, **345(1)**:495-501.
  18. Jenkins E, Moss JB, Pace JM, Bridgewater LC: **The new collagen gene COL27A1 contains SOX9-responsive enhancer elements.** *Matrix Biol* 2005, **24(3)**:177-184.
  19. Camper L, Hellman U, Lundgren-Akerlund E: **Isolation, cloning, and sequence analysis of the integrin subunit alpha10, a beta1-associated collagen binding integrin expressed on chondrocytes.** *J Biol Chem* 1998, **273(32)**:20383-20389.
  20. Bengtsson T, Aszodi A, Nicolae C, Hunziker EB, Lundgren-Akerlund E, Fassler R: **Loss of alpha10beta1 integrin expression leads to moderate dysfunction of growth plate chondrocytes.** *J Cell Sci* 2005, **118**:929-936.
  21. Kikuchi A, Okuhara M, Karikusa F, Sakurai Y, Okano T: **Two-dimensional manipulation of confluent cultured vascular endothelial cells using temperature-responsive poly(N-isopropylacrylamide)-grafted surfaces.** *J Biomater Sci Polym Ed* 1998, **9(12)**:1331-1348.
  22. Ochi M, Uchio Y, Kawasaki K, Wakitani S, Iwasa J: **Transplantation of cartilage-like tissue made by tissue engineering in the treatment of cartilage defects of the knee.** *J Bone Joint Surg Br* 2002, **84(4)**:571-578.
  23. Sato M, Asazuma T, Ishihara M, Kikuchi T, Masuoka K, Ichimura S, Kikuchi M, Kurita A, Fujikawa K: **An atelocollagen honeycomb-shaped scaffold with a membrane seal (ACHMS-scaffold) for the culture of annulus fibrosus cells from an intervertebral disc.** *J Biomed Mater Res A* 2003, **64(2)**:248-256.
  24. Okano T, Yamada N, Okuhara M, Sakai H, Sakurai Y: **Mechanism of cell detachment from temperature-modulated, hydrophilic-hydrophobic polymer surfaces.** *Biomaterials* 1995, **16(4)**:297-303.

Publish with **BioMed Central** and every scientist can read your work free of charge

"BioMed Central will be the most significant development for disseminating the results of biomedical research in our lifetime."

Sir Paul Nurse, Cancer Research UK

Your research papers will be:

- available free of charge to the entire biomedical community
- peer reviewed and published immediately upon acceptance
- cited in PubMed and archived on PubMed Central
- yours — you keep the copyright

Submit your manuscript here:  
[http://www.biomedcentral.com/info/publishing\\_adv.asp](http://www.biomedcentral.com/info/publishing_adv.asp)



# Noninvasive Evaluation of Tissue-Engineered Cartilage with Time-Resolved Laser-Induced Fluorescence Spectroscopy

Toshiharu Kutsuna, M.D.,<sup>1</sup> Masato Sato, M.D., Ph.D.,<sup>1</sup> Miya Ishihara, Ph.D.,<sup>2</sup>  
Katsuko S. Furukawa, Ph.D.,<sup>3-5</sup> Toshihiro Nagai, M.D., Ph.D.,<sup>1</sup> Makoto Kikuchi, M.D., Ph.D.,<sup>2</sup>  
Takashi Ushida, Ph.D.,<sup>3-6</sup> and Joji Mochida, M.D., Ph.D.<sup>1</sup>

Regenerative medicine requires noninvasive evaluation. Our objective is to investigate the application of time-resolved laser-induced fluorescence spectroscopy (TR-LIFS) using a nano-second-pulsed laser for evaluation of tissue-engineered cartilage (TEC). To prepare scaffold-free TEC, articular chondrocytes from 4-week-old Japanese white rabbits were harvested, and were inoculated at a high density in a mold. Cells were cultured for 5 weeks by rotating culture (RC) or static culture (SC). The RC group and SC group at each week ( $n = 5$ ), as well as normal articular cartilage and purified collagen type II (as controls), were analyzed by TR-LIFS. The peak wavelength was compared with those of type II collagen immunostaining and type II collagen quantification by enzyme-linked immunosorbent assay and tensile testing. The fluorescence peak wavelength of the TEC analyzed by this method shifted significantly in the RC group at 3 weeks, and in the SC group at 5 weeks ( $p < 0.01$ ). These results correlated with changes in type II collagen (enzyme-linked immunosorbent assay) and changes in Young's modulus on tensile testing. The results were also supported by immunohistologic findings (type II collagen staining). Our findings show that TR-LIFS is useful for evaluating TEC.

## Introduction

NONINVASIVE MEANS ARE ESSENTIAL for evaluating physical properties and tissue characterization of regenerative tissues for implantation. Our research group (Ishihara *et al.*) discovered that stress wave propagation and attenuation by pulsed laser irradiation was influenced by tissue elasticity and, based on this principle, proposed the use of photoacoustic measurement for viscoelastic characterization of biological tissue.<sup>1-5</sup> In this study, we investigated whether pulsed laser irradiation and measurement of excited autofluorescence would enable noninvasive real-time evaluation of viscoelasticity and tissue characterization. Autofluorescence is the basis for photodynamic therapy in malignant lesions, and photosensitizers were originally used. Photosensitizers cause tissue injury and remain in the body or tissue samples for certain periods of time, so they are not suitable for serial monitoring. In addition, they are not suitable for use in regenerative medicine, in which biocompatibility is required. In the late 1970s, background signals

that were previously thought to be exogenous fluorescence were found to be due to endogenous autofluorescence.<sup>6</sup> Since that time, the use of autofluorescence for detection and periodic screening of tumors and use in dental lesions, skin lesions, and atherosclerotic plaques have been described in many reports. The use of autofluorescence in regenerative medicine, however, is relatively recent, and few reports have described its application for evaluation of regenerative tissues.<sup>7</sup> Autofluorescent substances include structural proteins (collagen and elastin), amino acids (tryptophan, tyrosine, and phenylalanine), lipids (cholesterol), vitamins (vitamin A, D, and K), and enzyme cofactors (NAD(P)H, FAD).<sup>6,8-9</sup> The structure of these autofluorescent substances is reflected by their fluorescence spectra and lifetime (decay characteristics) in tissue. Thus, fluorescence spectral analysis allows us to predict tissue biochemical composition and metabolic activity.<sup>10,11</sup> Collagen, the major component of cartilage, is now recognized as an important autofluorescent substance. The same is true for enzyme cofactors NAD(P)H in cells.<sup>12</sup> The scaffold-free tissue-engineered cartilage (TEC) used in this

<sup>1</sup>Department of Orthopaedic Surgery, Surgical Science, Tokai University School of Medicine, Kanagawa, Japan.

<sup>2</sup>Department of Medical Engineering, National Defense Medical College, Tokorozawa, Saitama, Japan.

<sup>3</sup>Department of Bioengineering, <sup>4</sup>Biomedical Engineering Laboratory, Department of Mechanical Engineering, School of Engineering, and

<sup>5</sup>Center for Nanobio Integration, and <sup>6</sup>Division of Biomedical Materials and Systems, Center for Disease Biology and Integrative Medicine, Faculty of Medicine, University of Tokyo, Tokyo, Japan.



study was constructed as follows. Cartilage formation by secretion of molecules forming the extracellular matrix (ECM) by chondrocyte differentiation from aggregated mesenchymal cells during the embryonic development stage and dynamic stress is reproduced *in vitro* by a simple system of high-density seeding of cells in a cylindrical mold and rotating flow using a rotary shaker. Then, without specific growth factors, the dedifferentiated monolayer of cultured chondrocytes is redifferentiated in a three-dimensional (3D) culture without a scaffold, and their ability to produce matrix is reacquired. This TEC, based on cell distribution, tissue composition, and quantification of glycosaminoglycans and collagen, has tissue characteristics and physical properties that closely approximate those in normal cartilage.<sup>13–16</sup> Hyaline cartilage has a high moisture content, a sparse cell population, and a collagen and proteoglycan-rich ECM, and thus the autofluorescent substances in cartilage are primarily collagen and NAD(P)H correlating with cell components.<sup>8</sup> In addition, most of the collagen is type II, with trace amounts of types VI, IX, and XI.<sup>17</sup> Therefore, from production to postimplantation of TEC, the monitoring of chondrocyte differentiation and ECM production requires serial measurement of type II collagen and NAD(P)H. Our objective was to investigate the application of time-resolved laser-induced fluorescence spectroscopy (TR-LIFS) for serial monitoring of TEC by comparing the results of TR-LIFS of scaffold-free TEC with the results of conventional evaluation of articular cartilage, including tissue characterization and physical properties. Conventional tissue characterization and evaluation of physical properties of articular cartilage includes biochemical quantification (enzyme-linked immunosorbent assay [ELISA]) of type II collagen and immunostaining. Among the physical properties of articular cartilage, proteoglycans contribute primarily to compression characteristics, whereas type II collagen plays more of a role in tensile characteristics.<sup>18,19</sup> Therefore, we performed tensile testing. Our study showed good correlation between the results and suggests that TR-LIFS is useful for quality non-invasive evaluation of TEC.

## Materials and Methods

### TR-LIFS setup, spectroscopic measurements, and data analysis

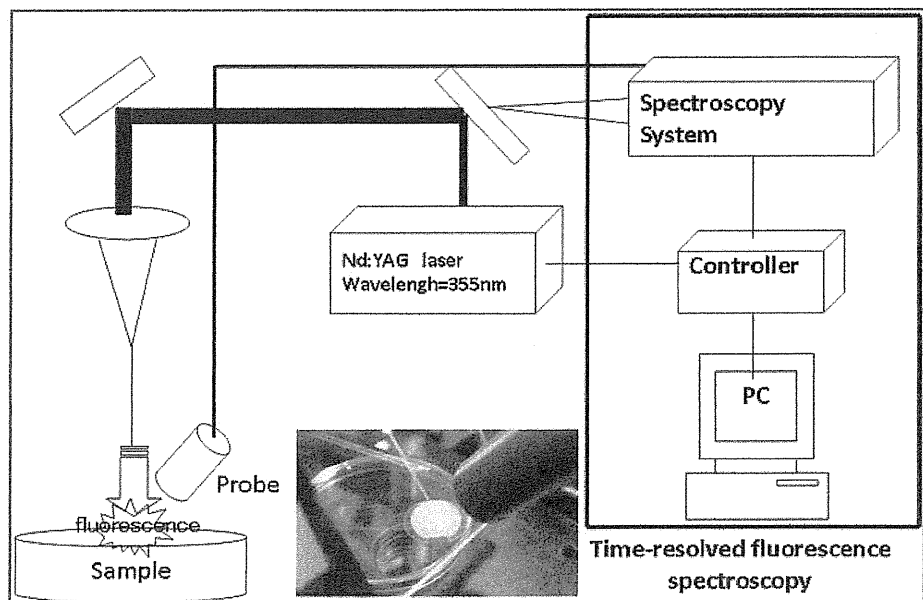
Figure 1 depicts the experimental setup. The beam was concentrated with a lens attached to a quartz fiber with a core diameter of 400  $\mu\text{m}$ . Fluorescence was induced using the third harmonic wave of a Q switch Nd:YAG laser (wavelength 355 nm, frequency 5 Hz). The pulsed laser was directed onto the sample at a 45° angle of incidence, with a beam diameter of about 5 mm, through a laser transmission optical fiber. Induced fluorescence was collected perpendicularly to this beam. Distance between the probe and sample was 20 mm. The output energy of the optical fiber was adjusted to 50  $\mu\text{J}/\text{pulse}$ ,<sup>3</sup> which is substantially lower than the biological damage threshold. Time-resolved fluorescent spectroscopy of the fluorescence induced by pulsed laser was obtained using a photonic multi-channel analyzer with an image intensifier detector coupled to a charge coupled device (CCD) camera (wavelength range, 200–860 nm; resolution, 3 nm; gate time, 10 ns). Samples were washed with purified water, and at room temperature, each sample was subjected to measurement at 10 locations.<sup>1–5</sup> We used a sharp cut filter to intercept excitation light (SCF-50S-38L; Sigma-Koki, Tokyo, Japan).

The measured fluorescence was displayed in 3D, and peak wavelength was used as parameters. All calculations were performed using MatLab software (MathWorks Inc., Natic, MA).

### Cell culture

Articular chondrocytes were harvested from the shoulders and knees of 4-week-old Japanese white rabbits weighing about 1 kg ( $n=12$ ). Cartilage was digested in Dulbecco's modified Eagle's medium (DMEM/F12; Gibco-Invitrogen, Carlsbad, CA) containing 0.4% (w/v) actinase E (Kaken Pharmaceutical, Tokyo, Japan) for 1 h, and in DMEM/F12 containing 0.016% (w/v) bacterial collagenase P (Roche

**FIG. 1.** System for fluorescent measurement. Time-resolved fluorescent spectroscopy was performed using a photonic multi-channel analyzer with a 4-Ch digital signal generator. The fluorescent features of the developed measurement system are as follows: wavelength range, 200–860 nm; wavelength resolution, <3 nm; exposure time, 19 ms; gate time, 10 ns. The parameters of measured fluorescence obtained using MatLab software were peak wavelength at fluorescence maximum, fluorescent spectral bandwidth at half-maximal amplitude (FWHM), and integrated intensity of time-resolved spectrum. Color images available online at [www.liebertonline.com/ten](http://www.liebertonline.com/ten).



Diagnosics GmbH, Mannheim, Germany) for 3 h. The digested cartilage was passed through a 70- $\mu$ m cell strainer (Becton Dickinson Labware, Franklin Lakes, NJ) and was centrifuged at 1500 rpm for 5 min. The pellet was suspended in DMEM/F12, 10% fetal bovine serum (Gibco, Invitrogen Corporation, Carlsbad, CA), 100 U/mL penicillin (Gibco), 100  $\mu$ g/mL streptomycin (Gibco), 0.25  $\mu$ g/mL fungizone (Gibco), and 50  $\mu$ g/mL ascorbic acid (Wako Pure Chemical Industries, Osaka, Japan). Chondrocytes were inoculated on 500-cm<sup>2</sup> dishes at  $1 \times 10^4$  cells/cm<sup>2</sup> and cultured at 37°C with 5% CO<sub>2</sub> and 95% humidity. After 1 week, the primary culture cells (P0) (70% confluence monolayer) were detached using 0.05% trypsin/EDTA (Gibco) at 37°C for 10 min. Cells were then washed with phosphate-buffered saline (PBS), resuspended in medium, and cultured at  $1 \times 10^4$  cells/cm<sup>2</sup> for two passages. Medium was replaced every 3 days.<sup>15,16</sup>

#### *Cartilage tissue formation*

Second-passage chondrocytes were resuspended at a density of  $1.0 \times 10^7$  cells/mL in DMEM/F12, 20% fetal bovine serum (Gibco), 100 U/mL penicillin (Gibco), 100  $\mu$ g/mL streptomycin (Gibco), 0.25  $\mu$ g/mL fungizone (Gibco), and 50  $\mu$ g/mL ascorbic acid (Wako Pure Chemical Industries). Cylindrical glass molds (diameter, 10 mm; height, 10 mm) were placed into a culture insert with a pore size of 0.4  $\mu$ m (Corning Costar Japan, Tokyo, Japan) to permit oxygen and nutrient diffusion. First, 15 mL of culture medium was added under the culture insert, and 15 mL of culture medium was added onto the culture insert. Next, 0.6 mL of the cell suspension was inoculated onto the mold, and was allowed to stand for 30 min. Gravity-assisted sedimentation of the cell suspension on the insert was confirmed, and about 30 mL of culture medium was then added to the culture insert until the mold was completely filled. This was cultured for 8 h at 37°C under 5% CO<sub>2</sub> and 95% humidity. The mold was then removed, and the cell mass (chondrocyte plate) with a form similar to the mold was cultured for 7 days under the same conditions. Constructs, shaped like the mold, were removed using a medicine spoon and moved to a nonadherent six-well culture dish, where they were cultured with 6 mL of medium per plate. Rotating culture (RC) was performed for 5 weeks using an orbital shaker (Taitec; 70 rpm; turn radius, 25 mm). Static culture (SC) and RC were performed at 37°C under 5% CO<sub>2</sub> and 95% humidity. Culture medium was replaced every 3 days.<sup>15,16</sup>

#### *Fixation and sectioning*

Samples were washed with PBS and fixed in 4% formalin solution. After ethanol dehydration, samples were immersed in isoamyl alcohol, embedded in paraffin, cut into 4- $\mu$ m sections, and stained with safranin-O and toluidine blue for proteoglycans. Sections were deparaffinized for immunohistochemistry using standard procedures. Sections were then treated with 0.005% proteinase (type XXIV; Sigma-Aldrich, St. Louis, MO) for 30 min at 37°C before incubation with primary antibody. After the slides were washed with PBS, endogenous peroxidase activity was blocked with 0.3% hydrogen peroxide in methanol for 15–20 min at room temperature. Next, sections were rinsed with PBS and incubated with normal goat serum (diluted 1:20 in PBS) for 30 min at room temperature. Primary mouse monoclonal antibody

directed against human collagen types I and II (Daiichi Fine Chemical, Toyama, Japan) was diluted 1:200 in PBS–1% bovine serum albumin (BSA; Sigma Aldrich, St. Louis, MO). Slides were incubated overnight at 4°C, washed 10 times with PBS, and incubated with biotin-conjugated goat anti-mouse secondary antibody (diluted 1:100 in PBS–1% BSA) in a humidified chamber for 1 h at room temperature. Slides were then treated with horseradish peroxidase-labeled streptavidin (streptavidin–horseradish peroxidase) for 1 h. Finally, slides were immersed in a 0.05% solution of diaminobenzidine in Tris-HCl buffer (pH 7.6) containing 0.005% hydrogen peroxide for 2–4 min until the color developed. To improve cell observation, the slides were counterstained with Mayer's hematoxylin. Transverse sections were observed and recorded with an inverted microscope and digital camera (objective lens,  $\times 20$ ).

#### *Biochemical analysis*

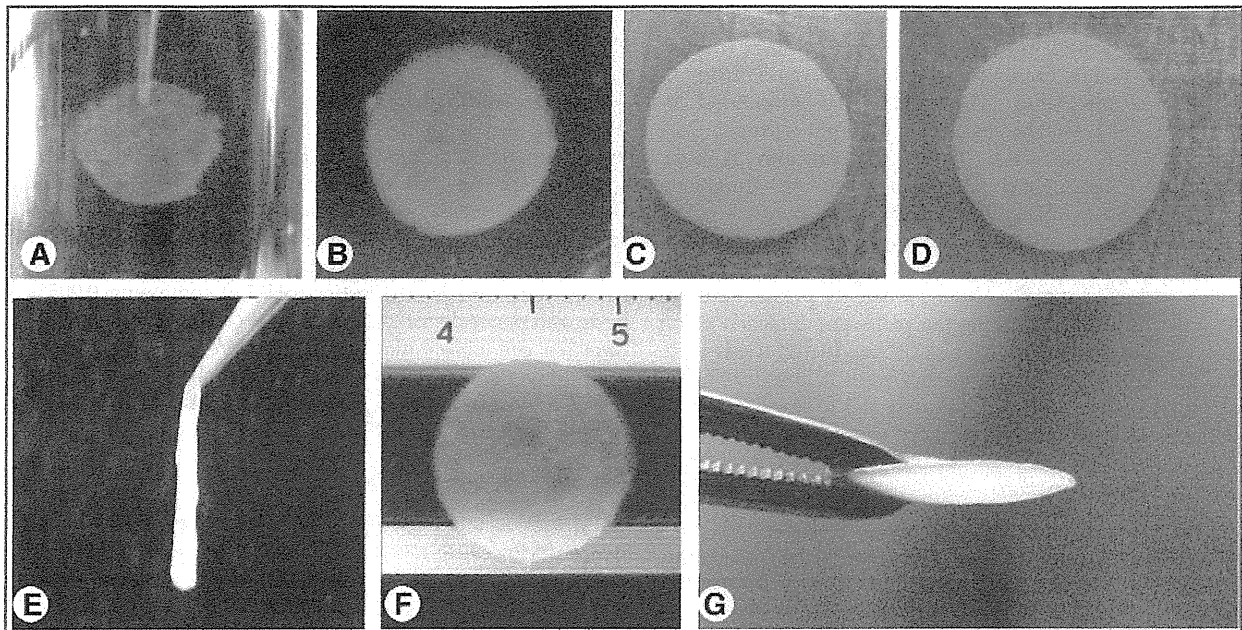
Type II collagen ELISA. Wet weight and weight after freeze-drying were measured to calculate moisture content. The freeze-dried sample and 0.5 mL of cold distilled water were added to an Eppendorf tube and incubated overnight at 4°C. The sample was centrifuged (10000 rpm, 3 min), and the supernatant was removed. Next, 0.5 mL of 3 M guanidine/0.5 M Tris-HCl (pH 7.5) was added to the sample tube, and this was mixed on a rotator/rocker overnight at 4°C. The sample was homogenized using a small electric homogenizer and centrifuged (10000 rpm, 3 min). The precipitate was washed with cold distilled water, and was then resuspended in 0.8 mL of 0.05 M acetic acid containing 0.5 M NaCl (adjusted to pH 2.9–3.0 with formic acid). Next, 0.1 mL of pepsin (10 mg/mL) dissolved in 0.05 M acetic acid was added and mixed, and this was incubated at 4°C for 48 h. Then, 0.1 mL of 10 $\times$ TBS (1.0 M Tris–2.0 M NaCl–50 mM CaCl<sub>2</sub>, pH 7.8–8.0) was added (adjusted to pH 8.0 with 1 N NaOH). In addition, 0.1 mL of pancreatic elastase (1 mg/mL dissolved in 1 $\times$ TBS, pH 7.8–8.0) was added, followed by mixing on a rotator/rocker overnight at 4°C. The sample was centrifuged (10000 rpm, 5 min), and the supernatant was collected. Type II collagen was assayed by ELISA (Native Type II Collagen ELISA Kit, Catalogue No. 6009; Chondrex NE, Redmond, WA) according to the manufacturer's protocol. ELISA samples were measured by spectrophotometry at 490 nm. The results were compared with the standard curve for type II collagen in the kit.

#### *Measurement of thickness and tensile properties*

Sample thickness was measured using a digital micrometer (minimum display, 0.001 mm; error,  $\pm 1 \mu$ m; degree of parallelization, 1  $\mu$ m). Tensile testing was performed with the sample set in a grip and at a pulling speed of 4 mm/min. Young's modulus was calculated from the slope of the linear portion of the load–deflection curve.

#### *Statistical analysis*

Samples were divided into the SC and RC groups, with comparisons at each week. All data are shown as means  $\pm$  standard error (SE). Factorial analysis of variance was used for comparisons. Each significant difference on analysis of variance was analyzed by multiple comparison using Scheffe's test. The level of statistical significance was  $p < 0.01$ .



**FIG. 2.** Macroscopic appearance of the chondrocyte plate, which formed after 7 days of primary static culture (SC) (A, E). Subsequently, a chondrocyte plate formed after rotating culture (RC) for 1 week (B, F), 2 weeks (G), 3 weeks (C), or 5 weeks (D). Scale bar = 1 mm. Color images available online at [www.liebertonline.com/ten](http://www.liebertonline.com/ten).

## Results

### Macroscopic appearance

The TEC after 1 week of primary SC retained a form similar to the mold (Fig. 2A). However, after removal from the culture medium, this shape could no longer be maintained (Fig. 2E). With RC and SC, thickness of the chondrocyte plate increased with culture duration (Fig. 2B–D). After 2 weeks of culture, the construct retained its shape even when handled with forceps (Fig. 2F, G).

### Histology and immunohistochemistry

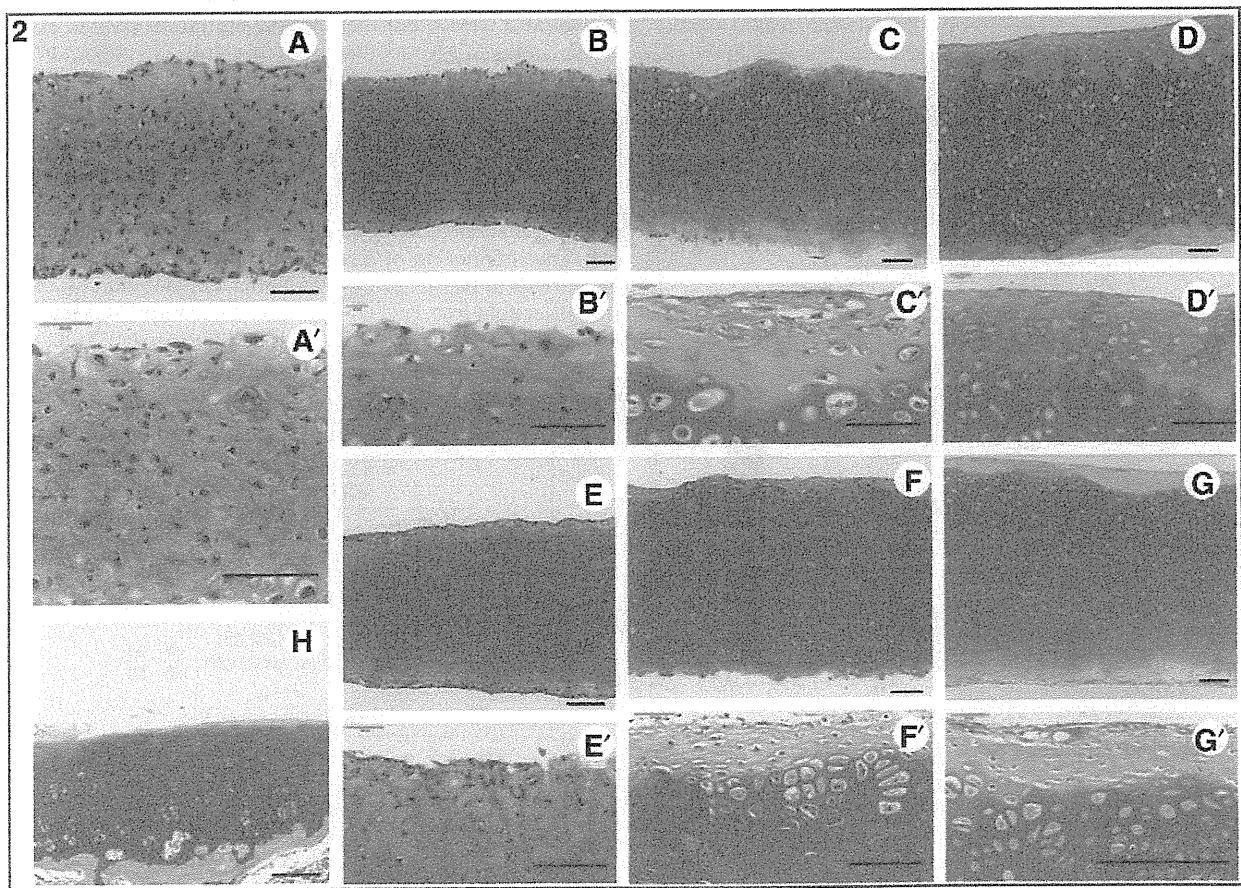
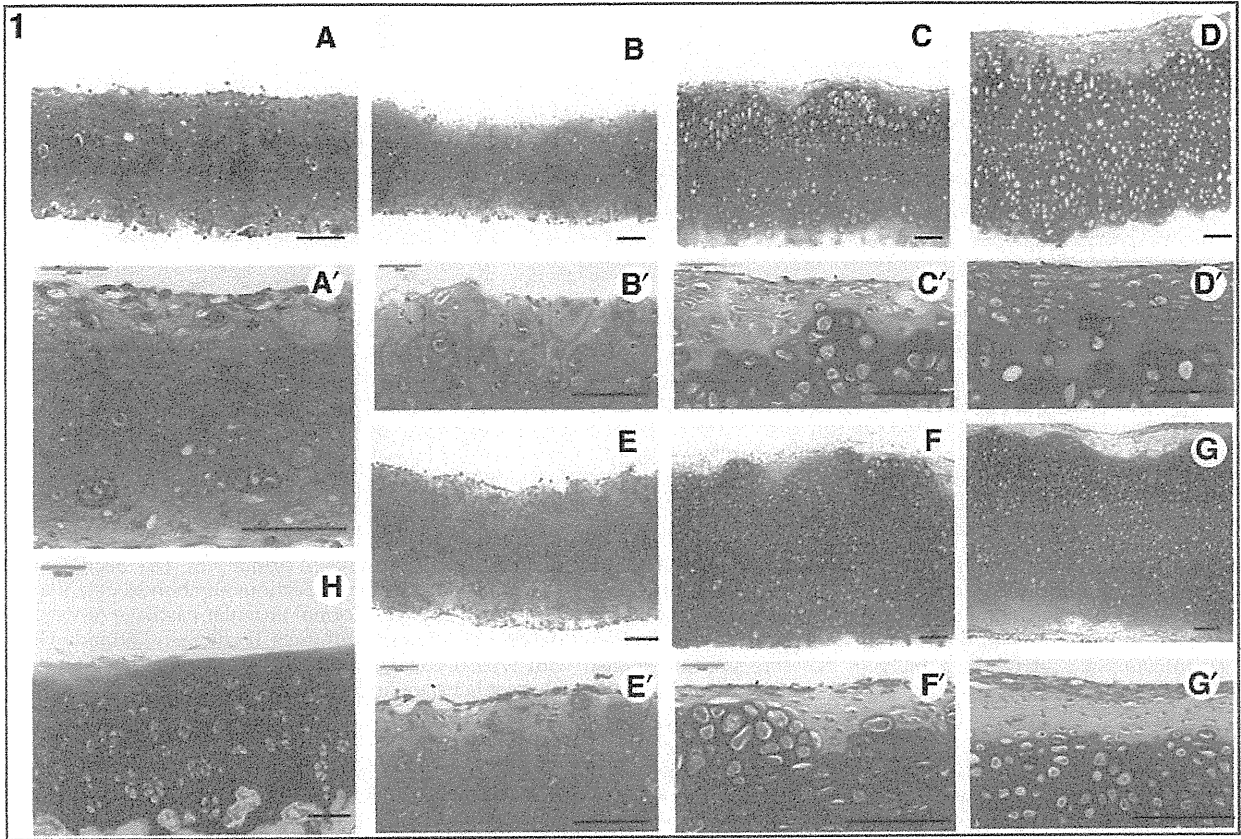
Figures 3-1H and 3-2H show the normal articular cartilage of knee from 4-week-old Japanese white rabbits. Figure 3-1A shows the toluidine blue staining during the primary 1 week of SC. Cells are uniformly distributed, and the ECM also stains uniformly. In the SCs at 1, 3, and 5 weeks (Fig. 3-1B, B', C, C', D, D'); as compared with rotational cultures at 1, 3, and 5 weeks (Fig. 3-1E, E', F, F', G, G'); cell distribution was uneven, cell density was lower, and numerous enlarged cells were observed. In addition, staining was uneven near the surface and, overall, tended to be weaker. On the other hand, in the rotational cultures at 1, 3, and 5 weeks (Fig. 3-1E, E', F, F', G, G'), cell distribution was uniform, and cell morphology was nearly uniform, with only a few enlarged cells. Further,

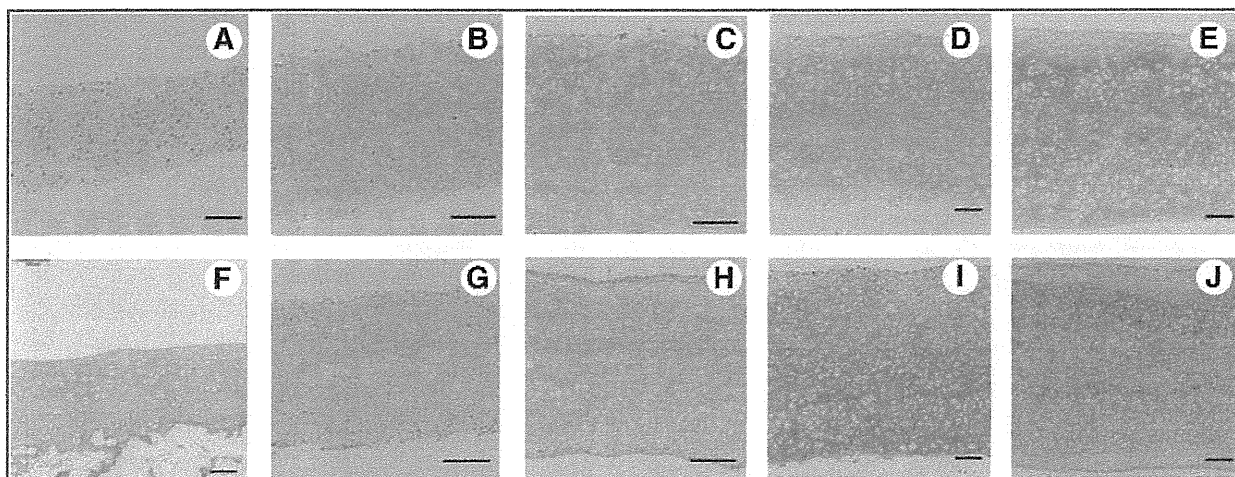
staining, with the exception of superficial fibroblastic cells, was uniform and tended to be stronger. The superficial fibrous layer, compared to the SCs (Fig. 3-1B, B', C, C', D, D'), was thicker and increased in thickness with culture duration (weeks). For the initial 1 week of SC, the SCs at 1, 3, and 5 weeks (Fig. 3-1B, B', C, C', D, D'), the rotational cultures at 1, 3, and 5 weeks (Fig. 3-1E, E', F, F', G, G'), and the staining characteristics for safranin-O were similar. In the SC group, immunostaining for type II collagen did not clearly differ up to 3 weeks of culture, but at 5 weeks of culture, staining was intense. In the RC group, staining did not clearly differ up to 2 weeks of culture, but staining was intense by 3 weeks of culture and remained so at week 5. In addition, overall staining for type II collagen, as compared to the SC group, tended to be more uniform and intense (Fig. 4). The results were similar to safranin-O and toluidine blue staining.

### Biochemical analysis

**Type II collagen ELISA.** Type II collagen content did not significantly differ between the groups at 2 weeks of culture, but at week 3 and later, type II collagen content was significantly greater in the RC group than in the SC group. In the SC group, there was no significant increase by 3 weeks, but the increase was significant at 5 weeks. In the RC group,

**FIG. 3.** Distribution of proteoglycans was investigated. Chondrocyte plate formed after 1 week of primary SC was stained with toluidine blue and safranin-O (1A, A', 2A, A'). Chondrocyte plate formed after 1, 3, and 5 weeks of SC was stained with toluidine blue and safranin-O (1B, B', C, C', D, D', 2B, B', C, C', D, D'). Chondrocyte plate formed after 1, 3, and 5 weeks of RC was stained with toluidine blue and safranin-O (1E, E', F, F', G, G', 2E, E', F, F', G, G'). Normal articular cartilage (4-week-old Japanese white rabbits) (1H, 2H). (A–H) Magnifications of objective lens,  $\times 4$ . (A'–G') Magnifications of objective lens,  $\times 20$ . Scale bar = 100  $\mu\text{m}$ . Color images available online at [www.liebertonline.com/ten](http://www.liebertonline.com/ten).





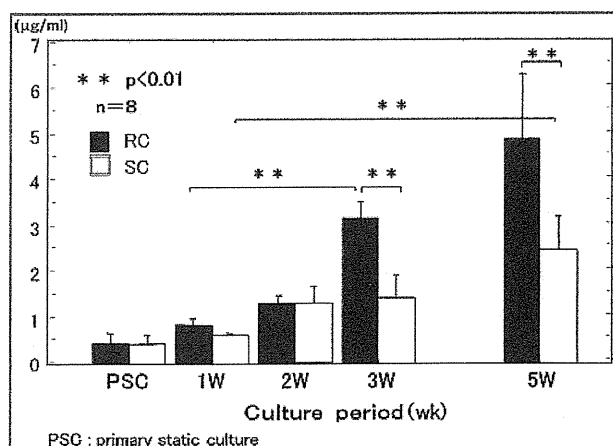
**FIG. 4.** Immunohistochemistry of paraffin sections of chondrocyte plate formed after 7 days of primary SC (A). Sections of chondrocyte plate formed after 1 week (B), 2 weeks (C), 3 weeks (D), and 5 weeks (E) of SC. Sections of chondrocyte plate formed after 1 week (G), 2 weeks (H), 3 weeks (I), and 5 weeks (J) of rotational culture. Normal articular cartilage (4-week-old Japanese white rabbits) (F). Chondrocyte plate at week 5 of SC was strongly stained with type II collagen antibody (E). Chondrocyte plates at weeks 3 and 5 of RC were strongly stained with type II collagen antibody (I, J). Magnifications of objective lens,  $\times 4$ . Scale bar = 100  $\mu\text{m}$ . Color images available online at [www.liebertonline.com/ten](http://www.liebertonline.com/ten).

there was no significant increase at 2 weeks, but by 3 weeks, there was a significant increase (Fig. 5).

#### Thickness and tensile properties

In both the RC and SC groups, thickness increased rapidly from 1 to 2 weeks. The rate of increase in thickness in the RC group was maintained up to week 5 of culture, whereas in the SC group, it tended to decrease (Fig. 6).

Young's modulus tended to increase after each week of culture in the RC group when compared with the SC group. In the SC group, there was no significant increase by 3 weeks, but the increase was significant at 5 weeks. In the RC group, there was no significant increase at 2 weeks, but the increase was significant by 3 weeks (Fig. 7).



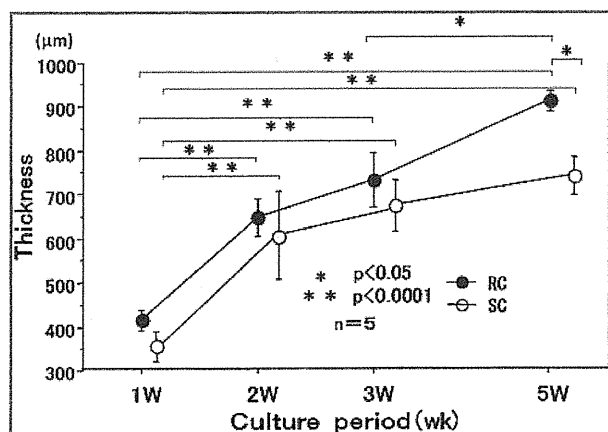
**FIG. 5.** Collagen type II expression of the chondrocyte plate during 5 weeks of culture was measured by enzyme-linked immunosorbent assay. Collagen type II expression was increased at 3 weeks of RC and at 5 weeks of SC. Error bars: standard error. PSC, primary SC.

#### Time-resolved laser-induced fluorescence spectroscopy

Changes were evaluated in peak wavelength at each week of culture of the TEC. In the SC group, there was no significant change at 3 weeks, but there was a significant change at 5 weeks. In the RC group, there was no significant change at 2 weeks, but at 3 weeks, there was a significant change (Fig. 8).

#### Discussion

The increasingly common clinical application of regenerative medicine has become a reality with advances in technology. Therefore, noninvasive methods are essential for real-time monitoring of tissue constructs, from the time of production to before, during, and after implantation. In our study, scaffold-free TEC was produced by simple RC, based on the principle that chondrocytes dedifferentiated in high-



**FIG. 6.** Time changes in thickness of the chondrocyte plate during 5-week RC. Thickness of the cartilage plate was measured using a digital micrometer.

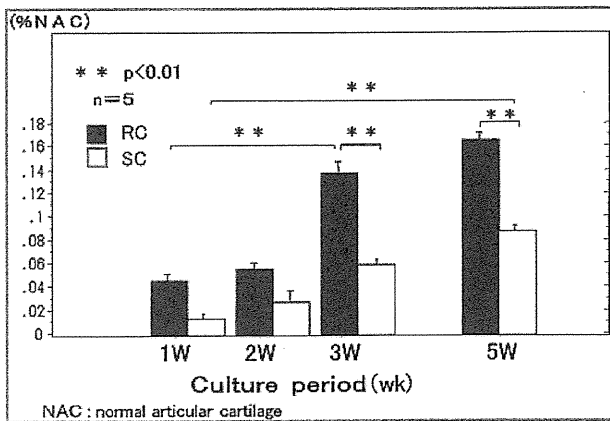


FIG. 7. Time changes in Young's modulus of the chondrocyte plate during 5 weeks of culture. Young's modulus of the chondrocyte plate was increased at 3 weeks of RC and at 5 weeks of SC. Error bars: standard error. NAC, normal articular cartilage.

density cell culture (due to cell-cell adhesions and interaction) will redifferentiate, and that mechanical stress is required for chondrocyte redifferentiation. Furukawa *et al.* and Nagai *et al.* have reported the usefulness of RC based on assays for proteoglycans, DNA, collagen, and collagen type I and II mRNA, and based on physical characteristics (tensile testing).<sup>13-16</sup> In our study, ELISA quantification of type II collagen also showed that RC significantly increased type II collagen production. These results were confirmed by fluorescence spectroscopy. Articular cartilage is hyaline cartilage, a tissue composed of about 2% chondrocytes and abundant ECM. ECM is composed of about 70% water, 20% collagen, and 10% proteoglycans or cell components. In addition, of the collagen that comprises 20% of hyaline cartilage, 80-90% is type II collagen. In other words, most articular cartilage tissue is type II collagen. The autofluorescence within the tissue is caused by collagen and coenzyme NAD(P)H in cell components. Thus, fluorescence emissions from cartilage are

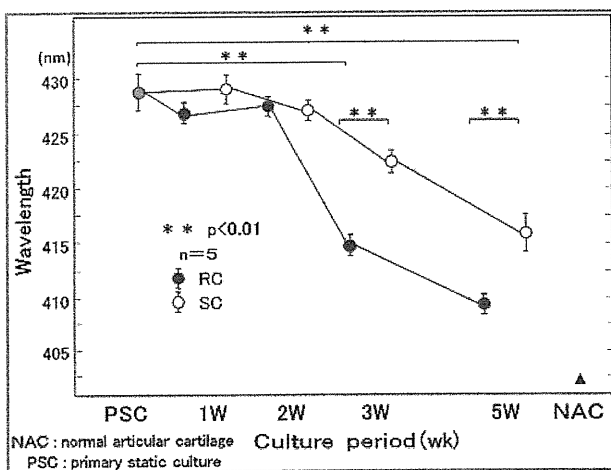


FIG. 8. Time changes in peak wavelength of the chondrocyte plate during 5-week RC. Peak wavelength of the chondrocyte plate decreased at 3 weeks of RC and at 5 weeks of SC.

mostly due to type II collagen. Type II collagen has attracted interest as an autofluorescent substance and for its important role in the viscoelastic properties of chondrocytes.<sup>9,18</sup> In our study, 5-week culture and serial fluorescence spectroscopy were performed. Changes in quantitative results and fluorescence peak wavelength of the TEC were compared. Type II collagen was significantly increased in the RC group at 3 weeks, and in the SC group at 5 weeks. Fluorescence peak wavelength also changed significantly in the RC group at 3 weeks (shifted to shorter wavelength), and in the SC group at 5 weeks. These findings indicate that in the RC group, type II collagen production was significantly increased as compared to the SC group. This occurred from weeks 2 to 3 of culture, and was easily discerned by changes in peak wavelength. Physical properties were also evaluated. Tensile strength of tissue generally correlated with collagen content, and compression strength generally correlated with proteoglycan content.<sup>18,19</sup> In this study, we measured tensile strength of the TEC. The results correlated both with changes in type II collagen content and changes in peak wavelength. Further, correlation analysis regarding type II collagen content, peak wavelength, and Young's modulus revealed significant correlations among all parameters. Peak wavelength reflected the type II collagen content of the sample, and it was clarified that it is possible to quantitatively evaluate the constituent representing the largest component ratio (Fig. 9). These results suggest the possibility of quantitatively evaluating other autofluorescent materials through analysis of the substance-specific fluorescence wavelength.

These changes also correlated with the immunostaining results for type II collagen. The peak wavelength data obtained by TR-LIFS were thought to reflect autofluorescence at the highest composition ratios among the sample autofluorescence substances. Tensile strength increased with culture duration (weeks); this increase corresponds to a rise in the type II collagen composition ratio.

The reason for the considerably lower strength, as compared to normal cartilage, is because tensile strength is influenced not only by type 2 collagen content but also by fiber orientation, tissue proteoglycan content, and cell density. In our study samples, Nagai, from our research group, measured proteoglycan (PG) content. This was markedly higher in 3-week cultures than in normal cartilage.<sup>15</sup> In addition, our study sample considerably has a higher cell density than has a normal articular cartilage tissue. Based on our results, changes in peak wavelength on fluorescence spectroscopy can be used to validate a tissue engineering cartilage culturing process. In 2004, Ashjian *et al.* measured autofluorescence of osteoinduced processed lipoaspirate cells (PLA) and performed a detailed analysis.<sup>16</sup> Spectroscopy of PLA cells not osteoinduced showed broad emission with a peak wavelength of 420-430 nm. This wavelength corresponded to the spectrum of skin-derived type I collagen and placenta-derived types IV and V collagen. Their results showed characteristics similar to the fluorescence spectrum of juvenile rabbit chondrocytes immediately after isolation. Although they reported no significant changes, spectroscopy of the osteoinduced PLA cells showed that the peak wavelength shifted toward 450 nm at 3, 5, and 7 weeks. This shift in peak wavelength was thought to indirectly represent differentiation of PLA cells to bone. They also analyzed the decay time using TR-LIFS and reported that spectroscopy of the osteoinduced PLA cells was

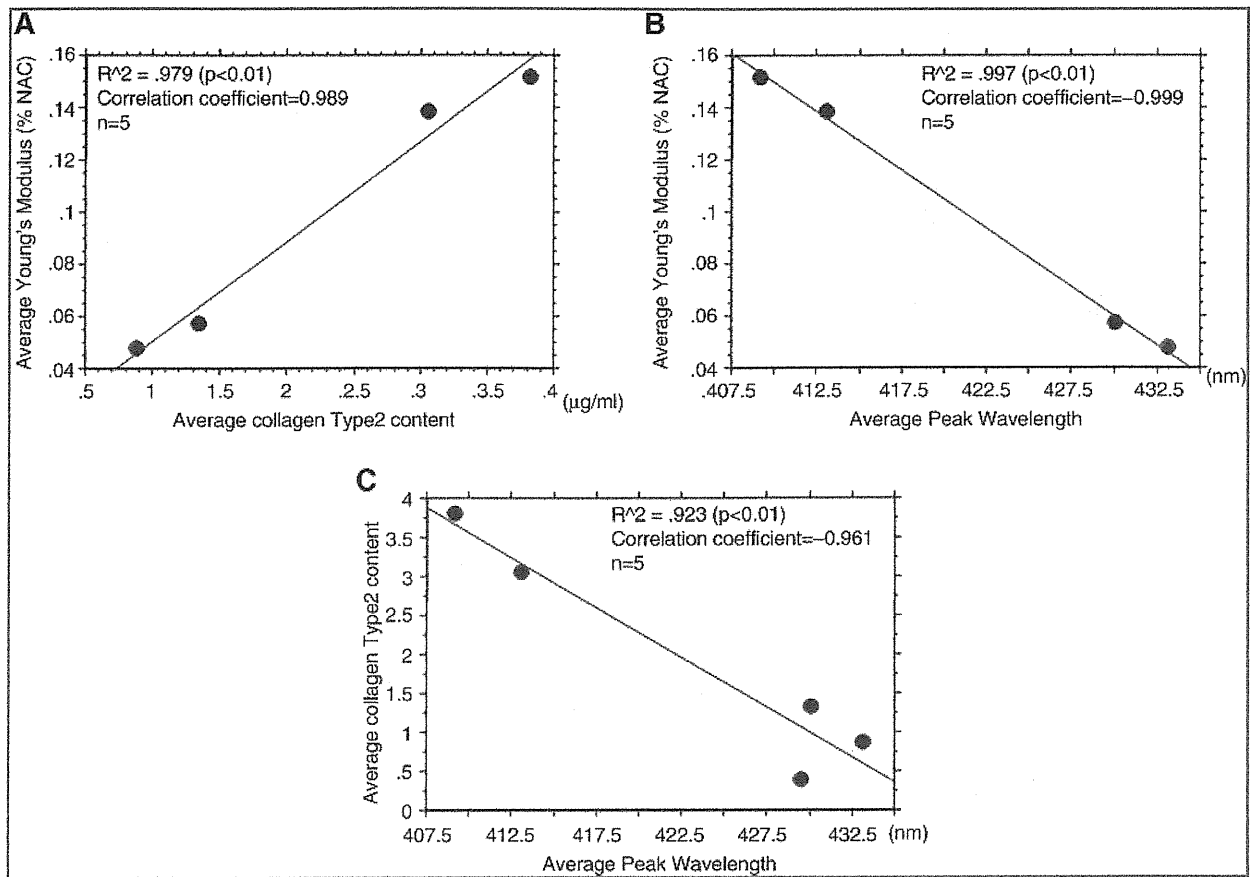


FIG. 9. (A) Correlation of average Young's modulus to average collagen type 2 content. (B) Correlation of average Young's modulus to average peak wavelength. (C) Correlation of average collagen type 2 content to average collagen peak wavelength.

characteristic for mainly type I collagen, and they stated that based on decay characteristics alone, collagen expression could be monitored. However, our study results suggest that when there is a specific tissue composition like hyaline cartilage, the changes in peak wavelength permit monitoring of type II collagen production. In addition, the serial changes in the fluorescence spectrum of osteoinduced PLA cells are similar to changes in the fluorescence spectrum associated with passages of juvenile rabbit chondrocytes in monolayer culture. Chondrocytes with a peak wavelength of 420–430 nm just after isolation that maintained differentiation produced collagen and formed TEC. The fluorescence peak wavelength shifted to 400 nm during culture, whereas the fluorescence peak wavelength of juvenile rabbit chondrocytes in monolayer culture shifted to 440–450 nm as the number passages increased (data not shown). At the excitation wavelength of NAD(P)H (290–350 nm), the fluorescence wavelength is 440–464 nm.<sup>20–22</sup> In addition, a decrease in collagen fluorescence and marked increase in NAD(P)H fluorescence have been reported with increased cell number and tissue dysplasia.<sup>20,23</sup> Therefore, the shift toward shorter wavelengths and the shift toward longer wavelengths represent collagen production when cell differentiation is maintained, and a decreased ability to produce collagen during cell dedifferentiation, respectively. When evaluating known tissue characteristics,

tissue autofluorescence can be identified by peak wavelengths alone. However, when detecting autofluorescence in unknown tissues, as noted, a shift toward a shorter peak wavelength does not necessarily indicate chondrogenesis, and a shift toward a longer peak wavelength does not necessarily indicate osteogenesis. For example, type I collagen from bovine Achilles tendon (peak 380 nm, decay time  $5.2 \pm 0.2$  ns) and calf skin (peak 420 nm, decay time  $1.05 \pm 0.1$  ns) have markedly different peak wavelengths and decay times.<sup>12</sup> If the peak wavelength of a tissue at the measurement start time is, for example, 390 nm, whether this is a shift to a longer wavelength representing chondrogenesis or osteogenesis cannot be assessed based on peak wavelength alone. In this case, assessing the decay time of each wavelength using TR-LIFS will help to distinguish chondrogenesis from osteogenesis based on lengthening or shortening. In our study, although the data are not shown, decay time was calculated, and characteristic lengthening or shortening of decay times at each wavelength was found based on culture duration (weeks) and culture method. For example, our data showed that the decay time of the type II collagen peak wavelength at 402 nm, with the initial SC (PSC1W) as a reference, shortened at week 1, was significantly prolonged at week 2, and remained the same at week 3. This finding suggests a process by which dedifferentiated monolayer cultured chondrocytes redifferentiate in a 3D cul-

ture, and to identify phenotypic modulations at a specific time, decay time must also be assessed. The above parameters must be comprehensively considered. When peak wavelength alone is used as a parameter, it can only be confirmed by the variability pattern. Thus, deviations from this variability pattern suggest a material that may not be ideal for regenerative tissue.

In our study, changes in fluorescence peak wavelength of the TEC were correlated with changes in type II collagen content. This demonstrates that monitoring changes in peak wavelength enables noninvasive evaluation of cartilage formation. This method of analysis may be useful in the advancing field of cartilage regenerative medicine.

### Acknowledgments

We thank Ms. Aya Saito, Ms. Mami Kokubo, and Ms. Tomoko Nakai for their expert technical assistance. This work was partially supported by New Energy and Industrial Technology Development Organization and Japan Foundation for Aging and Health.

### Disclosure Statement

No competing financial interests exist.

### References

- Ishihara, M., Sato, M., Sato, S., Kikuchi, T., Fujikawa, K., and Kikuchi, M. Viscoelastic characterization of biological tissue by photoacoustic measurement. *Jpn J Appl Phys* **42**, 556, 2003.
- Ishihara, M., Sato, M., Sato, S., Kikuchi, T., Fujikawa, K., and Kikuchi, M. Biomechanical characterization of tissue-engineered cartilages by photoacoustic measurement. *SPIE Proc* **4961**, 221, 2003.
- Ishihara, M., Sato, M., Sato, S., Kikuchi, T., Mochida, J., and Kikuchi, M. Usefulness of photoacoustic measurements for evaluation of biomechanical properties of tissue-engineered cartilage. *Tissue Eng* **11**, 1234, 2005.
- Ishihara, M., Sato, M., Kaneshiro, N., Mitani, G., Sato, S., Mochida, J., and Kikuchi, M. Development of a diagnostic system for osteoarthritis using a photoacoustic measurement method. *Lasers Surg Med* **38**, 249, 2006.
- Ishihara, M., Sato, M., Kaneshiro, N., Mitani, G., Sato, S., Ishihara, M., Mochida, J., and Kikuchi, M. Development of a noninvasive multifunctional measurement method using nanosecond pulsed laser for evaluation of regenerative medicine for articular cartilage. *SPIE Proc* **6084**, 30, 2006.
- de Veld, D.C.G., Witjes, M.J.H., van der Wal, J.E., Sterenborg, H.J.C.M., and Roodenburg, J.L.N. The status of *in vivo* autofluorescence spectroscopy and imaging for oral oncology. *Oral Oncol* **41**, 117, 2005.
- Ashjian, P., Elbarbary, A., Zuk, P., DeUgarte, D.A., Benhaim, P., and Hedrick, M.H. Noninvasive *in situ* evaluation of osteogenic differentiation by time-resolved laser-induced fluorescence spectroscopy tissue engineering. *Tissue Eng* **10**, 411, 2004.
- Georgakoudi, I., Jacobson, B.C., Muller, M.G., Sheets, E.E., Badizadegan, K., Carr-Locke, D.L., Crum, C.P., Boone, C.W., Dasari, R.R., Van Dam, J., and Feld, M.S. NAD(P)H and collagen as *in vivo* quantitative fluorescent biomarkers of epithelial precancerous changes. *Cancer Res* **62**, 682, 2002.
- Ramanujam, N. Fluorescence spectroscopy *in vivo*. In: Meyers, R.A., ed. *Encyclopedia of Analytical Chemistry*. Chichester, UK: John Wiley and Sons Ltd., 2000, pp. 20–56.
- Miller, E.J., and Gay, S. The collagens: an overview and update. *Methods Enzymol* **144**, 3, 1987.
- Fiorotti, R.C., Nicola, J.H., and Nicola, E.M.D. Native Fluorescence of oral cavity structures: an experimental study in dogs. *Photomed Laser Surg* **24**, 22, 2006.
- Marcu, L., Cohen, D., Maarek, J.M.I., and Grundfest, W.S. Characterization of type I, II, III, IV, and V collagens by time-resolved laser-induced fluorescence spectroscopy. *SPIE* **3917**, 93, 2000.
- Furukawa, K.S., Suenaga, H., Toita, K., Numata, A., Tanaka, J., Ushida, T., Sakai, Y., and Tateishi, T. Rapid and large-scale formation of chondrocyte aggregates by rotating culture. *Cell Transplant* **12**, 475, 2003.
- Furukawa, K.S., Imura, K., Tateishi, T., and Ushida, T. Scaffold-free cartilage by rotating culture for tissue engineering. *J Biotechnol* **133**, 134, 2008.
- Nagai, T., Furukawa, K.S., Sato, M., Ushida, T., and Mochida, J. Characteristics of a scaffold-free articular chondrocyte plate grown in rotating culture. *Tissue Eng* **14**, 1183, 2008.
- Nagai, T., Sato, M., Furukawa, K.S., Kutsuna, T., Ohta, N., Ushida, T., and Mochida, J. Optimization of allograft implantation using scaffold-free chondrocyte plates. *Tissue Eng* **14**, 1225, 2008.
- Mendler, M., Eich-Bender, S.G., Vaughan, L., Winterhalter, K.H., and Bruckner, P. Cartilage contains mixed fibrils of collagen type II, IX, and XI. *J Cell Biol* **108**, 191, 1989.
- Gemmiti, C.V., and Guldberg, R.E. Fluid flow increases type II collagen deposition and tensile mechanical properties in bioreactor-grown tissue-engineered cartilage. *Tissue Eng* **12**, 469, 2006.
- Poole, A.R., Kojima, T., Yasuda, T., Mwale, F., Kobayashi, M., and Laverty, S. Composition and structure of articular cartilage: a template for tissue repair. *Clin Orthop* **391**, S26, 2001.
- Lakowicz, J.R. *Principles of Fluorescence Spectroscopy*. New York: Plenum Press, 1999.
- Pradhan, A., Pal, P., Durocher, G., Villeneuve, L., Balassy, A., Babai, F., Gaboury, L., and Blanchard, L. Steady state and time resolved fluorescence properties of metastatic and non-metastatic malignant cells from different species. *J Photochem Photobiol B Biol* **3**, 101, 1995.
- Glassman, W.S., Steinberg, M., and Alfano, R.R. Time resolved and steady state fluorescence spectroscopy from normal and malignant cultured human breast cell lines. *Lasers in the Life Sciences* **6**, 91, 1994.
- Mayevsky, A., and Chance, B. Intracellular oxidation-reduction state measured *in situ* by a multichannel fiber-optic surface fluorometer. *Science* **217**, 537, 1982.

Address correspondence to:

Masato Sato, M.D., Ph.D.

Department of Orthopaedic Surgery

Surgical Science

Tokai University School of Medicine

143 Shimokasuya, Isehara

Kanagawa 259-1193

Japan

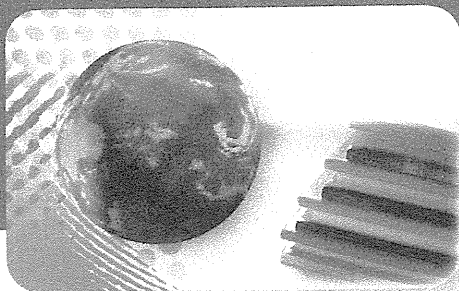
E-mail: sato-m@is.icc.u-tokai.ac.jp

Received: January 6, 2009

Accepted: July 9, 2009

Online Publication Date: February 3, 2010





# NOVA

Science Publishers, Inc.

DEVELOPMENT OF A DIAGNOSTIC  
SYSTEM FOR OSTEOARTHRITIS USING A  
PHOTOACOUSTIC MEASUREMENT METHOD  
AND TIME-RESOLVED AUTO-FLUORESCENCE

Masato Sato

Miya Ishihara

Genya Mitani

Toshiharu Kutsuna

Jeong Ik Lee

Makoto Kikuchi

Joji Mochida

In: "Bioengineering: Principles,  
Methodologies and Applications"

Editor: A. Garcia, C. Durand

ISBN: 978-1-60741-762-0 2010

400 Oser Avenue, Suite 1600  
Hauppauge, N. Y. 11788-3619  
Phone (631) 231-7269  
Fax (631) 231-8175  
E-mail: [Main@novapublishers.com](mailto:Main@novapublishers.com)  
<http://www.novapublishers.com>

*Chapter 7*

**DEVELOPMENT OF A DIAGNOSTIC SYSTEM FOR  
OSTEOARTHRITIS USING A PHOTOACOUSTIC  
MEASUREMENT METHOD AND TIME-RESOLVED  
AUTO-FLUORESCENCE**

*Masato Sato<sup>1\*</sup>, Miya Ishihara<sup>1,2</sup>, Genya Mitani<sup>1</sup>, Toshiharu  
Kutsuna<sup>1</sup>, Jeong Ik Lee<sup>1</sup>, Makoto Kikuchi<sup>2</sup>, Joji Mochida<sup>1</sup>*

<sup>1</sup> Department of Orthopaedic Surgery, Surgical Science, Tokai University School of  
Medicine, 143 Shimokasuya, Isehara, Kanagawa, 259-1193 Japan.

<sup>2</sup> Department of Medical Engineering, National Defense Medical College, 3-2 Namiki,  
Tokorozawa, Saitama, 359-8513 Japan.

**Key words:** Diagnostic system • Laser • Osteoarthritis • Photoacoustic measurement  
• Tissue-engineered cartilage

**ABSTRACT**

We have developed new methods to measure some essential properties of cartilage: a photoacoustic measurement method and time-resolved fluorescence spectroscopy. These can be used to evaluate the outcomes of tissue-engineered cartilage, regenerated articular cartilage tissue after surgery, and the degenerated cartilage of osteoarthritis patients. A nanosecond-pulsed laser, which is completely noninvasive, is focused onto the target cartilage and induces a photoacoustic wave, which will propagate with attenuation, which is affected by the viscoelasticity of the surrounding cartilage. The decay time during which the amplitude of the photoacoustic wave is reduced by a factor of 1/e is the key numerical value used to characterize and evaluate the viscoelasticity and rheological

---

\* Corresponding author:

Masato Sato, MD., PhD., Associate Professor and Research Director, Department of Orthopaedic Surgery, Surgical Science, Tokai University School of Medicine 143 Shimokasuya, Isehara, Kanagawa, 259-1193 Japan. Email: sato-m@is.icc.u-tokai.ac.jp, TEL: +81-463-93-1121 (ext 2320), FAX: + 81-463-96-4404

behavior of the cartilage. In this study, we also investigated whether pulsed laser irradiation and the measurement of excited autofluorescence allow us to noninvasively evaluate tissue characters in real time. Our findings show that time-resolved laser-induced fluorescence spectroscopy is useful for evaluating tissue-engineered cartilage. This measurement system, predicated on the interactions between optics and living organs, is a suitable methodology for diagnosis during arthroscopy, because it allows the quantitative and multidirectional evaluation of the original function of the cartilage based on a variety of parameters.

## INTRODUCTION


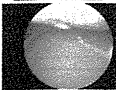

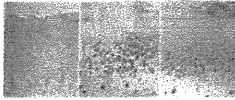
Osteoarthritis, which is thought to affect 24 million people in Japan [1], is not a direct threat to life. However, it both affects the activities of daily living and diminishes the quality of life of sufferers, so the associated human and social loss cannot be overestimated. The disease involves dysfunction caused by cartilage degeneration, but no objective evaluation methodologies based on the original function of the articular cartilage are currently available. Evaluations that are made to establish conservative therapies or the prognosis of surgery as a treatment for osteoarthritis are merely based on the patients' subjective symptoms or the degree of narrowing of the joint space on X-ray images. It is important to accurately measure and quantitatively evaluate the mechanical characteristics of the cartilage (viscosity, elasticity, and lubrication), and the tissue properties of the original articular cartilage to understand the pathological condition in detail and to judge the treatment effects. Therefore, the development of such an evaluation technology is required to facilitate a functional diagnosis of osteoarthritis (Table 1). If it is possible to do this noninvasively, then it should be possible to accurately understand the pathologies and plan and undertake treatments for locomotor apparatus diseases that accompany the degeneration of cartilage, such as osteoarthritis. It will also be useful as an objective evaluation methodology in clinical trials of new drugs, etc. It should thus be possible to better understand the pathological condition in detail and to make a prognosis based on a body of clinical data. This in turn will facilitate the careful planning of treatments according to pathological conditions of individual patients, improving their activities of daily living and enhancing the lives of many people. We propose the application of a unique measurement and evaluation methodology [2–15], which we have developed *in vitro* to noninvasively assess regenerating cartilage (tissue-engineered cartilage) and to diagnose cartilage degeneration.

## SUPERIORITY OF THE USE OF LASER

The scattering, reflection, and increase in temperature attributable to absorption and the production of fluorescence and acoustic waves are regarded as the main effects when light or laser beams irradiate living organs to be measured (Figure 1) [12]. A noninvasive and selective diagnostic device that uses optics via an optical fiber has recently attracted attention. It is based on a technology that takes advantage of the interactions between optics and living organs. The use of these interactions makes possible the simultaneous collection of not only morphological information but also various physiological and biochemical data, so its

potential for use as a diagnostic device is greater than that of techniques based on a single type of information, such as ultrasonic waves. Bioinstrumentation and imaging with a laser beam, which have recently attracted attention, have features that facilitate the application of this technology to the medical field (Table 2). We focused on the interactions between living organs and optics, especially photoacoustic waves and fluorescence, measured a variety of parameters related to these interactions when induced by the same laser, and developed a system that allows the simultaneous evaluation of the mechanical characteristics and properties of tissue (Figure 2) [3–5].

**Table 1. Comparison of the Evaluation Methods**

The conventional methods to evaluate articular cartilage		To evaluate the essential functions of articular cartilage
1. Joint space loss (X ray diagnosis)		1. Viscoelastic characteristics → Photoacoustic measurement (Arthroscopic examination)
2. Appearance of the cartilage surface (Arthroscopic examination)		2. Characterization of extracellular matrix → Time-resolved autofluorescence spectroscopy (Arthroscopic examination)
3. Probing (Arthroscopic examination)		3. Lubricating behavior → difficult to measure <i>in vivo</i>
4. Histological assessment (Biopsy)		

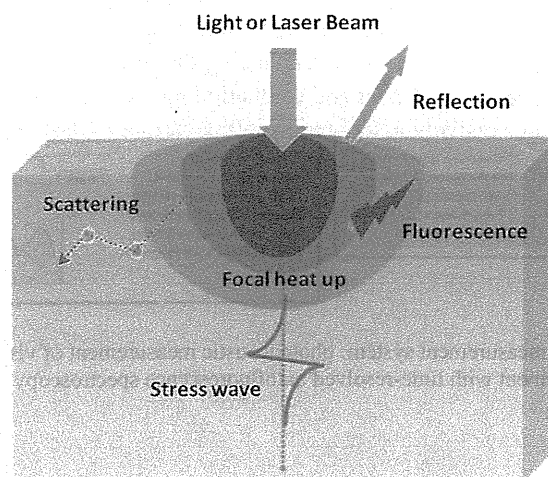


Figure 1. Mutual interaction between light and a living body